ACS OMEGA

http://pubs.acs.org/journal/acsodf

Article

Preparation and Electrochemical Characterization of La and Al Co-doped NCM811 Cathode Materials

Mingyu Zhang, Chaoyong Wang, Junkai Zhang, Gang Li, and Li Gu*

Cite This: *ACS Omega* 2021, 6, 16465−16471

Read Online

ACCESS | Metrics & More | Article Recommendations

ABSTRACT: $LiNi_{0.8}Co_{0.1}Mn_{0.1}O_2$ (NCM811) became a research hot point because of its low cost, environmental friendliness, and excellent electrochemical performance. However, Li^+/Ni^{2+} intermixing is an essential factor affecting its applicability. Doping could be an important method to improve the electrochemical performance of NCM811-based cathode materials. In this work, La and Al co-doped NCM811 was prepared by a solid-state method. Results from X-ray diffraction (XRD), scanning electron microscopy (SEM), and energy-dispersive spectroscopy (EDS) and electrochemical performance were discussed in depth. These showed that when La and Al doping concentrations were 1 and 0.5%, the samples showed the best performance. The as-improved performances were mainly attributed to the reduced Li^+/Ni^{2+} intermixing, suppressed phase transition, and decreased potential polarization and impedance.

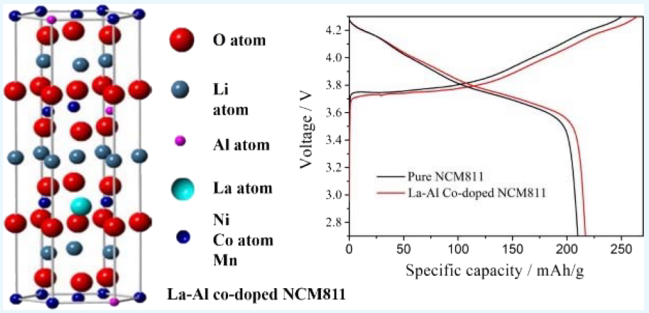

1. INTRODUCTION

Ni-rich $LiNi_xCo_yMn_{1-x-y}O_2$ ($x > 0.6$) have been applied in lithium-ion batteries (LIBs) as cathode materials with low environmental pollution, high energy density, good rate performance, and long cycle life. However, significant Li^+/Ni^{2+} intermixing can be obtained as the active Ni content in $LiNi_{0.8}Co_{0.1}Mn_{0.1}O_2$ (NCM811) is as high as 0.8. Furthermore, as Ni^{2+} (0.69 Å) and Li^+ (0.76 Å) have close radii, Ni^{2+} could easily enter the Li vacancies of the Li layer, which could degrade the cycle performance seriously.[1−3]

For NCM811, Li^+/Ni^{2+} intermixing is an essential factor that can affect the initial discharge capacity loss and cycle performances. Ni^{2+} could be oxidized to Ni^{3+} with Jahn−Teller distortion during discharging, causing partially layered structure collapse and hindering the insertion/extraction of Li^+ ions.[2] Furthermore, during the cycle, the anisotropy on the lattice scale will cause the primary particles to crack at the grain boundary, reducing the ionic conductivity between the primary particles and causing an electrolyte flow into the cracks of the primary particles. This aggravates the side reaction between the active material and electrolyte and increases the EIS layer resistance (R_{sf}).[4] Kondrakov et al. found that the lattice constant decreased from 14.469 to 13.732 Å during Li^+ extraction, making it difficult to embed Li^+, while the discharging cycle performance decreased.[5]

Many studies have shown that doping could be an efficient approach to improve the electrochemical performance of NCM811-based cathode materials.[6] Cation doping can efficiently reduce the Li^+/Ni^{2+} intermixing and enhance the stability of the crystal structure. Generally, a dopant with a larger radius can increase the distance between crystal layers and increase the diffusion rate of Li^+.[7] In addition, a dopant with a strong bond energy between transition metals can reduce the dissolution of transition metals and escape lattice oxygen, improving stability and safety.[8] Several dopants like La,[7] Nb,[6] Ti,[9] Cr,[10] Ca,[11] Zr,[12] W,[13] Mg,[14] K,[15] P,[16] and S[17] have been successfully explored to enhance the electrochemical properties of NCM811.

Dong et al. obtained a La-doped NCM811 cathode material by using the co-precipitation method.[7] The results showed that La^{3+}entered the lattice to occupy Ni^{2+} sites. Thus, the capacity retention rate was as high as 95.2% after 100 cycles at 2.8−4.3 V (1 C). Du et al. found that when the Ti doping amount was 2%, the initial discharge capacity reached 205.7 mAh/g (2.8−4.5 V at 0.5 C), and the capacity retention rate was 86.9% after 200 cycles (1 C).[9] Li et al. investigated the effect of Cr doping on NCM811 and found that Cr^{6+} could inhibit Li^+/Ni^{2+} intermixing and Jahn−Teller distortion, stabilizing the structure.[10] When the Cr^{6+} content was 1%, the discharge capacity of NCM811 was 209.9 mAh/g at 2.7−4.3 V (0.1 C).

Received: March 26, 2021
Accepted: June 2, 2021
Published: June 15, 2021

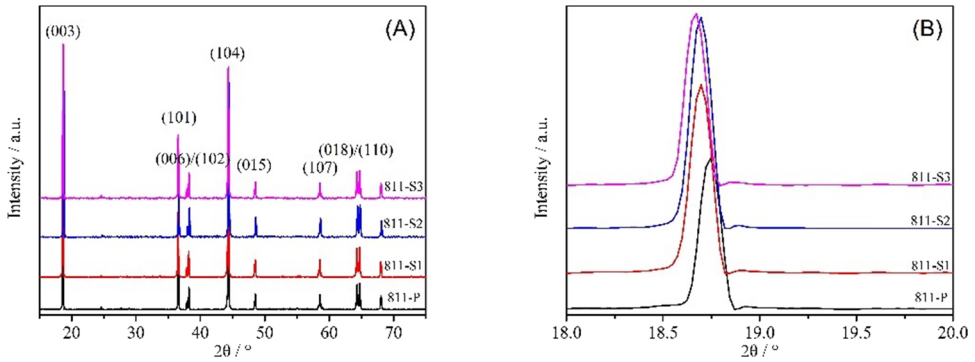

Figure 1. (A) XRD patterns and (B) zoomed-in XRD patterns of pure and La^{3+}−Al^{3+} co-doped NCM811 cathode materials.

Chen et al. prepared Ca-doped NCM811 by a solid-state method.[11] When the doping amount was 6%, the capacity retention rate was 81.10% after 50 cycles at 2.8−4.3 V (0.5 C). Min et al. studied the electrochemical performances of Al−Mg co-doped NCM811.[18] The results showed that Mg^{2+} doping could reduce the degree of cation disorder, while Al^{3+} doping can inhibit the formation of oxygen vacancies. Yue et al. prepared $LiNi_{0.8}Co_{0.1}Mn_{0.1}O_{2-z}F_z$ by sintering prepared NCM811 with NH_4F at 450 °C for 5 h.[8] The results showed that F doping could effectively inhibit HF corrosion and improve crystal structure and cycle performance. The capacity retention rate was 94.3% after 100 cycles at 2.8−4.3 V (2 C).

Besides, because single-component doping can only improve usually just one parameter, multicomponent doping was then widely considered.[19] For example, Naghash and Lee confirmed that phase structure stability could be significantly enhanced by Mg doping, but the rate performance was reduced.[20] On the other hand, Liang et al. used Mg and Al as co-dopants to inhibit the formation of oxygen vacancies, restrain phase transformation, and decrease cation mixing to improve the specific capacity and cycle stability.[21] Similarly, La and Al co-doping was successfully applied to enhance the high-voltage and high-energy-density properties of $LiCoO_2$.[22]

The liquid method has been widely employed to prepare NCM cathode materials; however, the liquid route is disadvantageous because it is both time- and energy-consuming. The solid-state method is also suitable for the mass production of cathode materials. The lithium source can be mixed with transition metal sources in a strict stoichiometry at the beginning.[23] Recently, the development of single crystalline particles of NCM had enabled long lifetimes and high coulomb efficiency, as reported by Trevisanello et al.[24] Therefore, in this paper, La−Al co-doped NCM811 was prepared by the solid-state method to reduce Li^+/Ni^{2+}cation intermixing and to suppress phase transition with the aim of improving the cycle stability of NCM811.

2. EXPERIMENTS

La^{3+} and Al^{3+} co-doped $LiNi_{0.8-x}Co_{0.1}Mn_{0.1-y}O_2$ cathode materials were prepared by a previously described solid-state method.[25] According to the molar ratio of 1.05:0.8:0.1:0.1:x:y, a certain amount of LiOH, NiO, Co_3O_4, MnO_2, Al_2O_3, and La_2O_3 was weighed, respectively. All the raw materials were obtained from Aladdin Industrial Corporation (AR grade). After ball-milling, the powders were heated first to 650 °C for 4 h and subsequently to 860 °C for 20 h in an oxygen atmosphere to obtain $LiNi_{0.8-x}Co_{0.1}Mn_{0.1-y}O_2$. Corresponding to doping concentrations, the samples were marked as 811-P ($x = y = 0$), 811-S1 ($x = y = 0.25\%$), 811-S2 ($x = 0.25\%$, $y = 0.5\%$), and 811-S3 ($x = 0.5\%$, $y = 0.1\%$), respectively.

Then, the PVDF, carbon black, and NCM811 cathode materials were mixed with a mass ratio of 1:1:8 in NMP to obtain the slurry. Furthermore, the slurry was coated on the Al foil and dried at 110 °C under vacuum for 12 h. The coated Al foil was then punched into discs (diameter 15 mm), and the weight of the NCM811 active material on each disc was about 2.1−2.3 mg. Finally, the cathode electrodes were assembled into coin cells with an electrolyte ($LiPF_6$), separator (Celgard), and anode (Li metal) in a glove box.

X-ray diffraction (XRD, XRD-7000, Japan) was used to investigate the crystal structure using a Cu Kα radiation in the 2θ range of 10−80°. A scanning electron microscope (SEM, JSM-5400F, Japan) coupled with an energy-dispersive spectroscope (EDS) was used to observe the morphology and the element distribution. The charge/discharge tests were performed on a battery test system (CT2001A, Landian, China) in the voltage of 2.7−4.3 V. The cyclic voltammetry (CV) and the electrochemical impedance spectroscopy (EIS) were acquired by an electrochemical workstation (CHI660E, Chinstruments, China).

3. RESULTS AND DISCUSSION

3.1. Phase Structure and Morphology. Figure 1 shows the XRD patterns of La^{3+}−Al^{3+} co-doped NCM811. It can be observed that the positions and intensities of all the diffraction peaks for various samples are following the standard pattern (PDF: 74-0919) with a typical α-$NaFeO_2$ hexagonal layered structure and $R3m$ space group. Furthermore, no detectable impurities can be observed, indicating that La^{3+} and Al^{3+} were successfully embedded and introduced as dopants into the NCM811 lattice. Both (006)/(102) and (018)/(110) peaks of pure and doped samples showed significant cleavage, indicating that La^{3+}−Al^{3+} co-doping did not influence the layered structure.

Table 1. Lattice Parameters of Pure and La^{3+}−Al^{3+} Co-doped NCM811 Cathode Materials

sample	a (Å)	c (Å)	c/a	R = (003)/(104)
811-P	2.8736	14.2072	4.9440	1.1178
811-S1	2.8787	14.2164	4.9384	1.2104
811-S2	2.8762	14.2213	4.9444	1.2287
811-S3	2.8754	14.2242	4.9468	1.1213

The lattice parameters of pure and co-doped samples are shown in Table 1. With the increasing La^{3+} content, the c value

https://doi.org/10.1021/acsomega.1c01552
ACS Omega 2021, 6, 16465−16471

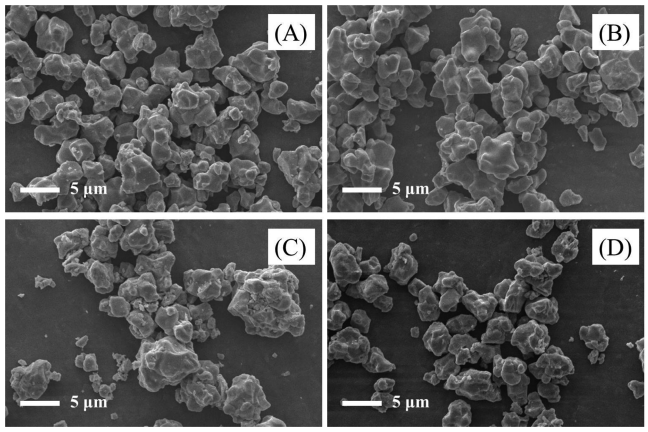

Figure 2. SEM micrographs of La^{3+}−Al^{3+} co-doped NCM811 samples: (A) 811-P, (B) M811-S1, (C) 811-S2, and (D) 811-S3.

gradually increases. This could happen as the ion radius of La^{3+} (1.03 Å) is much larger than that of Ni^{2+} (0.69 Å), leading to an expanded interlayer spacing. At the same time, c/a values of both pure and co-doped samples were large (>4.899), indicating a well-arranged layered structure.[26] Generally, the R value ((003)/(104)) is an important parameter used to characterize the degree of Li^{+}/Ni^{2+} intermixing. It can be observed that this value first increased and then decreased as the amount of doping agent increased. Sample 811-S2 showed the highest R value, indicating that an appropriate amount (La = 0.25%, Al = 0.5%) of doping could reduce the cation intermixing.

To investigate the influence of La^{3+}−Al^{3+} co-doping on the morphology of NCM811, SEM micrographs were taken (Figure 2). The particle sizes of all samples were relatively uniform without apparent agglomeration. Furthermore, all the co-doped samples' morphology remained quasi-unchanged,

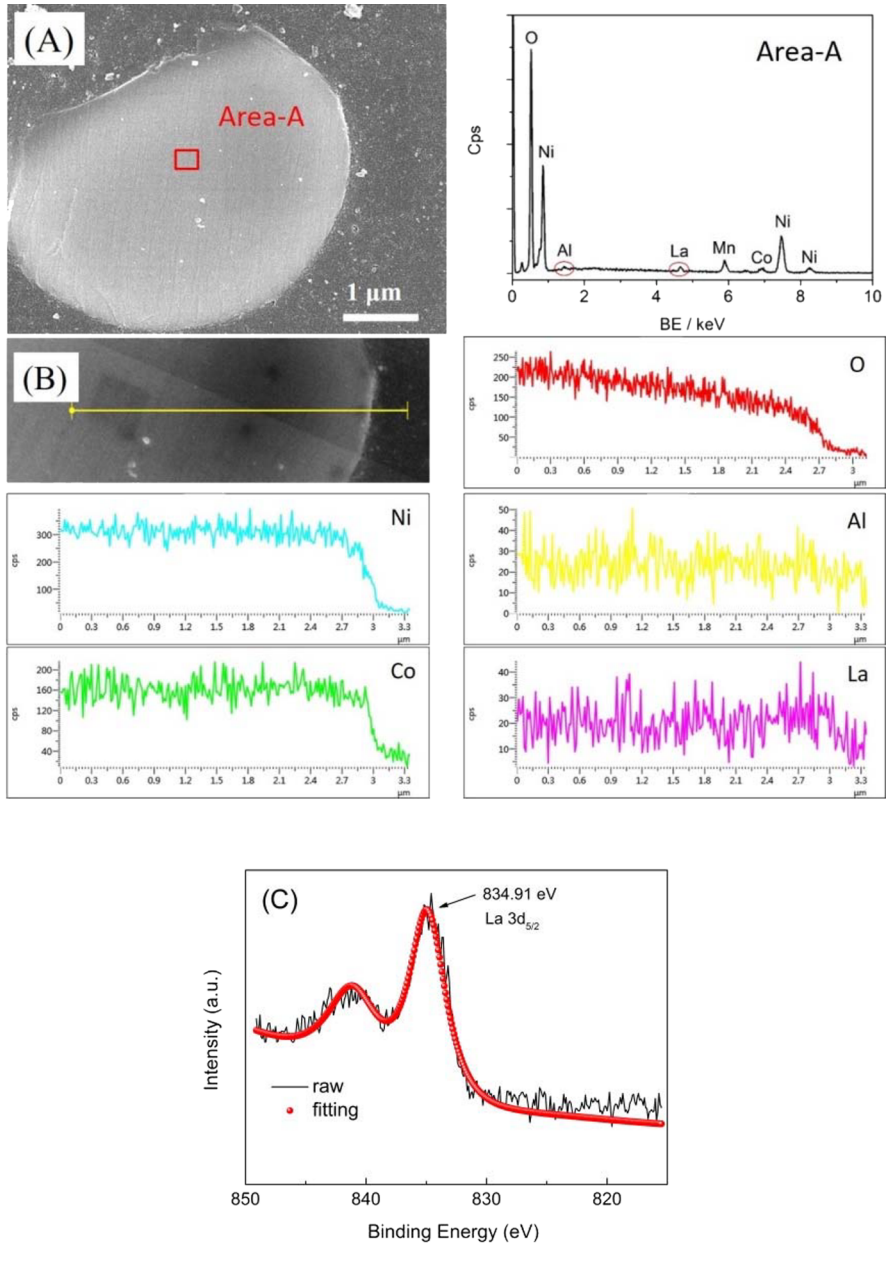

Figure 3. EDS investigation (A and B) and high-resolution La 3d XPS spectra (C) of sample 811-S2.

https://doi.org/10.1021/acsomega.1c01552
ACS Omega 2021, 6, 16465−16471

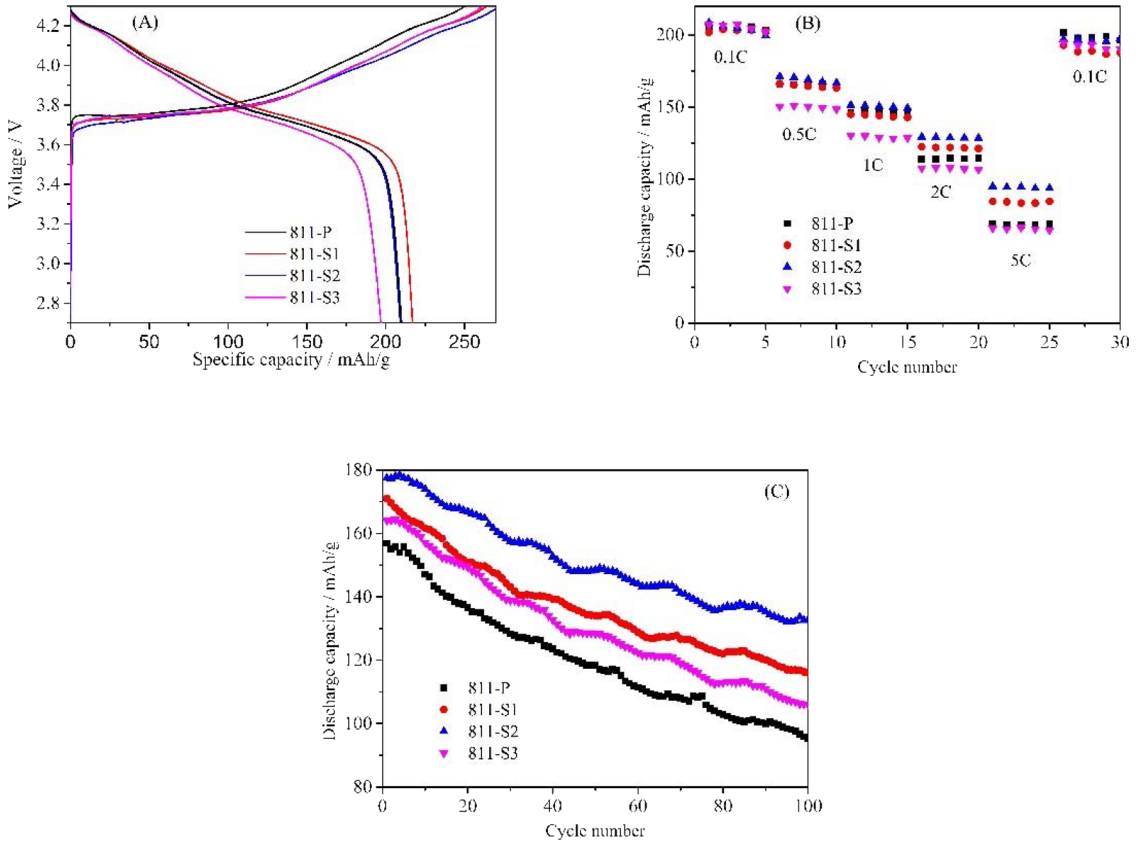

Figure 4. Initial charge/discharge performances at 0.05 C (A), rate performances (B), and cycling performances at 1 C (C) of pure and co-doped samples.

Table 2. Initial Charge/Discharge Specific Capacities of La^{3+}−Al^{3+} Co-doped NCM811-Based Samples at 0.05 C

sample	811-P	811-S1	811-S2	811-S3
charge capacity (mAh/g)	252.2	263.8	273.5	260.1
discharge capacity (mAh/g)	196.6	209.8	218.6	211.5

demonstrating that the introduction of La^{3+} and Al^{3+} had little effect on the morphology of the NCM811 cathode material.

The EDS analysis was performed on the cross section of sample 811-S2 particle to verify that the doping with La^{3+} and Al^{3+} was successful (Figure 3), which confirmed that the loading amount of Al^{3+} and La^{3+} in this sample was about 0.21 and 0.53%, respectively. According to these results, La and Al elements were uniformly distributed, indicating that La^{3+} and Al^{3+} were successfully doped into the NCM811. Moreover, XPS was carried out to explore the valence state of La dopant. The state of La was discussed in Figure 3C, where the peak at 834.91 eV corresponded to $3d_{5/2}$ of La^{3+}.

3.2. Charge/Discharge Performances. Figure 4 A shows the as-obtained samples' initial charge/discharge performances at 0.05 C in the range of 2.7−4.3 V (corresponding data are shown in Table 2). The initial specific discharge capacity increased and then decreased as the doping amount increased. Sample 811-S2 displayed the highest initial discharge specific capacity of 216.8 mAh/g, while the initial discharge specific capacity of the undoped sample 811-P was only 196.6 mAh/g. The results indicated that appropriate La^{3+} and Al^{3+} co-doping could effectively increase the initial discharge specific capacity. This is because La^{3+} doping with a large radius can enhance the diffusion of Li^{+}, improving the structural stability of NCM811 and efficiently strengthening the insertion/extraction process

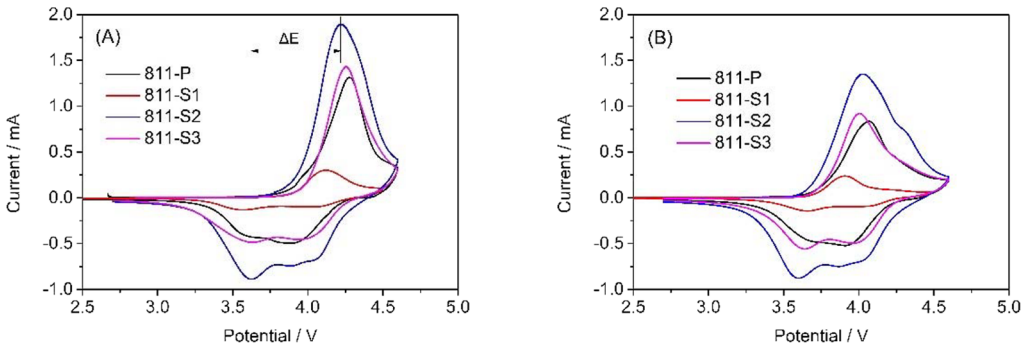

Figure 5. Cyclic voltammetry profiles of La^{3+}−Al^{3+} co-doped NCM811 samples: (A) the first cycle and (B) the second cycle.

https://doi.org/10.1021/acsomega.1c01552
ACS Omega 2021, 6, 16465−16471

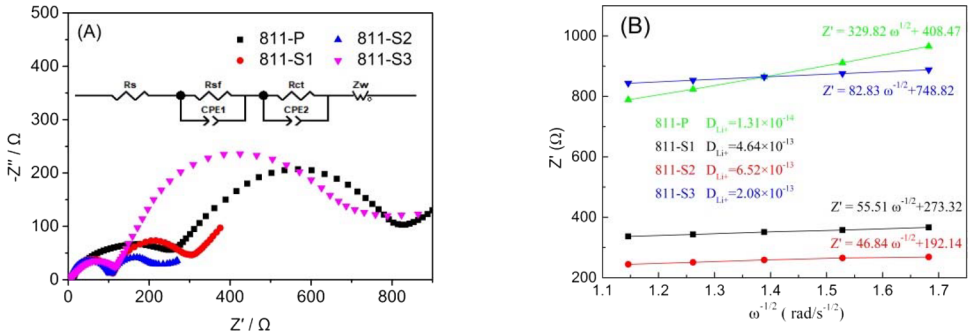

Figure 6. EIS curves of La^{3+}−Al^{3+} co-doped NCM811 samples (A) and the $Z'-\omega^{-1/2}$ relationship (B).

Table 3. Equivalent Resistance Values of La^{3+}−Al^{3+} Co-doped NCM811

sample	R_s (Ω)	R_{sf} (Ω)	R_{ct} (Ω)
811-P	4.2	223.6	546.8
811-S1	4.1	99.8	145.3
811-S2	4.8	82.5	116.7
811-S3	3.6	136.8	635.5

of Li^+.[18] Similarly, it was also reported that Al^{3+} could replace the Mn^{4+} site. Thus, it can promote the conversion of Ni^{2+} to Ni^{3+}, reducing the ratio of $Ni^{2+}/(Ni^{2+} + Ni^{3+})$ and decreasing the degree of Li^+/Ni^{2+} intermixing.[27]

The rate performances of samples are shown in Figure 4B. Although pure and La^{3+}−Al^{3+} co-doped samples displayed the same performance at a low rate (0.1 C), the discharge specific capacity of co-doped samples was much higher than that of undoped as the discharge current increased (2−5 C). For example, the discharge specific capacity of sample 811-S2 was 98.7 mAh/g, while that of the pure sample was only 48.7 mAh/g at 5 C. This is due to the La^{3+} and Al^{3+} co-dopants on the layered structure and crystal development of the NCM811 cathode material.

Figure 4C presents the cycling performances at 1 C in the range of 2.7−4.3 V. The highest initial discharge capacity belongs to sample 811-S2 (178.6 mAh/g at 1 C), while samples 811-P, 811-S1, and 811-S3 showed 148.2, 168.9, and 159.8 mAh/g, respectively. After 100 cycles, the discharge specific capacity of sample 811-S2 was 134.6 mAh/g, with a capacity retention of 75.4%. However, the capacity retention of samples 811-P, 811-S1, and 811-S3 were only 61.8, 68.5, and 67.6%, respectively (values obtained after 100 cycles at 1 C). Consequently, it can be affirmed that the proper amount of La^{3+} and Al^{3+} co-dopants can improve the cycle performances of the NCM811 cathode material. This can be attributed mainly to three factors. Firstly, La^{3+} doping with a large radius enhanced the insertion/extraction of Li^+ and decreased the charge/discharge process' impedance. Secondly, La^{3+} has a stronger affinity with oxygen, which can inhibit the loss of lattice oxygen and produce fewer oxygen vacancies. Therefore, the doped cathode material's layered structure became more stable, which is beneficial to the cycle performance.[7] Thirdly, Al^{3+} could act as a positive charge center that can promote the diffusion of Li^+. Besides, the intermixing degree of Li^+/Ni^{2+} was reduced due to the substitution of Al^{3+} for Mn^{4+}, decreasing the proportion of $Ni^{2+}/(Ni^{2+} + Ni^{3+})$ and ensuring the order of the NCM811 layered structure.[11]

3.3. Electrochemical Performances. Figure 5 shows the cyclic voltammetry curves of NCM811-based samples. All samples have two pairs of redox peaks at 3.9 and 4.2 V. The corresponding reduction peaks can be found around 3.6 and 4.1 V. According to previous reports, the largest redox peak observed in the range of 3.6−4.0 V could be attributed to the Ni^{2+}/Ni^{3+} or Ni^{4+} transition.[28] The other pair of redox peaks could be attributed to Co^{3+}/Co^{4+}.[29] As we know, a smaller voltage difference between the oxidation and reduction peaks indicates smaller potential polarization and better electrochemical reversibility of the cathodic material. The voltage difference between the redox peaks of 811-P, 811-S1, 811-S2, and 811-S3 samples was 0.65, 0.54, 0.52, and 0.66 V. The voltage difference between the redox peaks of 811-S2 was the smallest, showing outstanding reversibility.

The second circle of oxidation peak was observed to shift to a lower potential due to the SEI layer formation. The offset voltage value of 811-P was 0.28 V, while this value of sample 811-S2 was as low as 0.18 V. This indicates that the SEI layer of sample 811-S2 is much thinner than in the case of 811-P during the charge/discharge processes, which could enhance the insertion/extraction of Li^+. In summary, the appropriate amount of La^{3+} and Al^{3+} can reduce the potential polarization of NCM811, improving the reversibility and the cycle performance. The CV results are in good agreement with the XRD patterns (Figure 1), initial charge/discharge performance, and cycle performance (Figure 4).

Figure 6 presents the EIS curves of La^{3+}−Al^{3+} co-doped NCM811, while the inset presents the equivalent circuit. The Z-View software was used to fit the experimental data, and the corresponding impedance values are shown in Table 3. The impedance of the co-doped sample was significantly reduced. The EIS layer's resistance (R_{sf}) and the charge transfer resistance (R_{ct}) of sample 811-S2 were only 82.5 and 116.7 Ω, respectively. Simultaneously, the R_{sf} and R_{ct} values of the undoped sample 811-P were 223.6 and 546.8 Ω, respectively. This shows that the proper amount of La^{3+} and Al^{3+} co-doping can reduce the impedance of NCM811, increasing the conductivity. Besides, Al^{3+} as a positive charge center also promotes the diffusion of Li^+. However, as the amount of doping agent increases, the samples' R_{sf} and R_{ct} values increase as well. This is also because the radius of La^{3+} is relatively large: if the doping amount is too large, the lattice distortion increases and the order of the layered structure decreases, increasing the cathode's impedance. Moreover, the diffusion coefficients of lithium-ion (D_{Li}^+) in the cathodes were calculated from the slopes of the fitted lines in Figure 6B; sample 811-S2 showed the highest D_{Li}^+ (6.52×10^{-13}). This is because the La^{3+} doping with a large radius increases the interlayer spacing, which is beneficial to the insertion/extraction of Li^+.

https://doi.org/10.1021/acsomega.1c01552
ACS Omega 2021, 6, 16465−16471

4. CONCLUSIONS

La^{3+} and Al^{3+} co-doped NCM811 materials were successfully synthesized via a solid-state reaction. The effects of doping concentrations on the phase structure, micromorphology, and electrochemical performance of NCM811 were discussed in depth. The results showed that when La and Al doping concentrations were 0.25 and 0.5%, the sample showed the best performance in terms of capacity and retention. The initial discharge specific capacity was 218.6 mAh/g (0.05 C) and 178.6 mAh/g (1 C). After 100 cycles at 1 C, the discharge specific capacity was 134.6 mAh/g with 75.4% capacity retention. These excellent performances were assigned to the low cation intermixing, stable structure, and low potential polarization and impedance during the charge/discharge process after co-doping with La and Al.

AUTHOR INFORMATION

Corresponding Author

Li Gu − *Sino-German Robotics School, Shenzhen Institute of Information Technology, Shenzhen 518172, China*; Email: guli@sziit.edu.cn

Authors

Mingyu Zhang − *School of Information Engineering, Jilin Engineering Normal University, Changchun 130052, China*; orcid.org/0000-0003-0272-6588

Chaoyong Wang − *School of Information Engineering, Jilin Engineering Normal University, Changchun 130052, China*

Junkai Zhang − *Key Laboratory of Functional Materials Physics and Chemistry of the Ministry of Education, Jilin Normal University, Siping 136000, China*; orcid.org/0000-0002-6407-6173

Gang Li − *Dali University, Dali 671003, China*

Complete contact information is available at: https://pubs.acs.org/10.1021/acsomega.1c01552

Notes

The authors declare no competing financial interest.

ACKNOWLEDGMENTS

This work was supported by the National Natural Science Foundation of China (11904128 and 32060308) and Doctoral Initiated Research Foundation Project under Grant BSKJ201822.

REFERENCES

(1) Jiang, J.; Du, K.; Cao, Y.; Peng, Z.; Hu, G.; Duan, J. Syntheses of spherical $LiMn_2O_4$ with Mn_3O_4 and its electrochemistry performance. *J. Alloys Compd.* **2013**, *577*, 138−142.

(2) Wu, F.; Tian, J.; Su, Y.; Wang, J.; Zhang, C.; Bao, L.; He, T.; Li, J.; Chen, S. Effect of Ni^{2+} content on lithium/nickel disorder for Ni-rich cathode materials. *ACS Appl. Mater. Interfaces* **2015**, *7*, 7702−7708.

(3) Tan, X.; Zhang, M.; Li, J.; Zhang, D.; Yan, Y.; Li, Z. Recent progress in coatings and methods of Ni-rich $LiNi_{0.8}$ $Co_{0.1}Mn_{0.1}O_2$ cathode materials: A short review. *Ceram. Int.* **2020**, *46*, 21888−21901.

(4) Myung, S.-T.; Maglia, F.; Park, K.-J.; Yoon, C. S.; Lamp, P.; Kim, S.-J.; Sun, Y.-K. Nickel-Rich layered cathode materials for automotive lithium-ion batteries: achievements and perspectives. *ACS Energy Lett.* **2017**, *2*, 196−223.

(5) Kondrakov, A. O.; Geßwein, H.; Galdina, K.; de Biasi, L.; Meded, V.; Filatova, E. O.; Schumacher, G.; Wenzel, W.; Hartmann, P.; Brezesinski, T.; Janek, J. Charge transfer-induced lattice collapse in Ni-rich NCM cathode materials during delithiation. *J. Phys. Chem. C* **2017**, *121*, 24381−24388.

(6) Li, J.; Zhang, M.; Zhang, D.; Yan, Y.; Li, Z. An effective doping strategy to improve the cyclic stability and rate capability of Ni-rich $LiNi_{0.8}Co_{0.1}Mn_{0.1}O_2$ cathode. *Chem. Eng. J.* **2020**, *402*, 126195.

(7) Dong, M.-x.; Li, X.-q.; Wang, Z.-x.; Li, X.-h.; Guo, H.-j.; Huang, Z. J. Enhanced cycling stability of La modified $LiNi_{0.8-x}Co_{0.1}Mn_{0.1}La_xO_2$ for Li-ion battery. *Trans. Nonferrous Met. Soc. China* **2017**, *27*, 1134−1142.

(8) Yue, P.; Wang, Z.; Wang, J.; Guo, H.; Xiong, X.; Li, X. Effect of fluorine on the electrochemical performance of spherical $LiNi_{0.8}Co_{0.1}Mn_{0.1}O_2$ cathode materials via a low temperature method. *Powder Technol.* **2013**, *237*, 623−626.

(9) Du, R.; Bi, Y.; Yang, W. C.; Peng, Z.; Liu, M.; Liu, Y.; Wu, B.; Yang, B.; Ding, F.; Wang, D. Improved cyclic stability of $LiNi_{0.8}Co_{0.1}Mn_{0.1}O_2$ via Ti substitution with a cut-off potential of 4.5V. *Ceram. Int.* **2015**, *41*, 7133−7139.

(10) Li, L. J.; Wang, Z. X.; Liu, Q. C.; Ye, C.; Chen, Z. Y.; Gong, L. Effects of chromium on the structural, surface chemistry and electrochemical of layered $LiNi_{0.8-x}Co_{0.1}Mn_{0.1}Cr_xO_2$. *Electrochim. Acta* **2012**, *77*, 89−96.

(11) Chen, M.; Zhao, E.; Chen, D.; Wu, M.; Han, S.; Huang, Q.; Yang, L.; Xiao, X.; Hu, Z. Decreasing Li/Ni disorder and improving the electrochemical performances of Ni-rich $LiNi_{0.8}Co_{0.1}Mn_{0.1}O_2$ by Cadoping. *Inorg. Chem.* **2017**, *56*, 8355−8362.

(12) GAO, S.; ZHAN, X.; CHENG, Y. T. Structural, electrochemical and Li-ion transport properties of Zr-modified $LiNi_{0.8}Co_{0.1}Mn_{0.1}O_2$ positive electrode materials for Li-ion batteries. *J. Power Sources* **2019**, *410-411*, 45−52.

(13) Xiao, Z.; Zhou, C.; Song, L.; Cao, Z.; Jiang, P. Dual-modification of WO3-coating and Mg-doping on $LiNi_{0.8}Co_{0.1}Mn_{0.1}O_2$ cathodes for enhanced electrochemical performance at high voltage. *Ionics* **2021**, *27*, 1909−1917.

(14) Liu, J.; Zou, Z.; Zhong, S.; Zhang, S.; Zhang, H. Improved electrochemical performance of magnesium-doped $LiNi_{0.8-x}Mg_xCo_{0.1}Mn_{0.1}O_2$ by CTAB-assisted solvothermal and calcining method. *Ionics* **2021**, *27*, 1501−1509.

(15) Xu, T.; Liu, C.; Guo, Z.; Li, W.; Li, Y.; Yang, G. Improved rate and cyclic performance of potassium-doped nickel-rich ternary cathode material for lithium-ion batteries. *J. Mater. Sci.* **2021**, *56*, 2399−2411.

(16) Yuan, A.; Tang, H.; Liu, L.; Ying, J.; Tan, L.; Tan, L.; Sun, R. G. High performance of phosphorus and fluorine co-doped $LiNi_{0.8}Co_{0.1}Mn_{0.1}O_2$ as a cathode material for lithium ion batteries. *J. Alloys Compd.* **2020**, *84*, 156210.

(17) Nanthagopal, M.; Santhoshkumar, P.; Shaji, N.; Sim, G. S.; Park, J. W.; Senthil, C.; Lee, C. W. An encapsulation of nitrogen and sulphur dual-doped carbon over Li $[Ni_{0.8}Co_{0.1}Mn_{0.1}]O_2$ for lithium-ion battery applications. *Appl. Surf. Sci.* **2020**, 145580.

(18) Min, K.; Seo, S. W.; Song, Y. Y.; Lee, H. S.; Cho, E. A first-principles study of the preventive effects of Al and Mg doping on the degradation in $LiNi_{0.8}Co_{0.1}Mn_{0.1}O_2$ cathode materials. *Phys. Chem. Chem. Phys.* **2017**, *19*, 1762−1769.

(19) Liang, C.; Kong, F.; Longo, R. C.; Zhang, C.; Nie, Y.; Zheng, Y.; Cho, K. Site-dependent multi component doping strategy for Ni-rich $LiNi_{1-2y}Co_yMn_yO_2$(y=1/12) cathode materials for Li-ion batteries. *J. Mater. Chem. A* **2017**, *5*, 25303−25313.

(20) Naghash, A. R.; Lee, J. Y. Lithium nickel oxy fluoride $(Li_{1-z}Ni_{1+z}F_yO_{2-y})$ and lithium magnesium nickel oxide $(Li_{1-z}(Mg_xNi_{1-x})_{1+z}O_2)$ cathodes for lithium rechargeable batteries: Part I. Synthesis and characterization of bulk phases. *Electrochim. Acta* **2001**, *46*, 2293−2304.

(21) Liang, Y.; Li, S.; Xie, J.; Yang, L.; Li, W.; Li, C.; Ai, L.; Fu, X.; Cui, X.; Shangguan, X. Synthesis and electrochemical characterization of Mg−Al co-doped Li-rich Mn-based cathode materials. *New J. Chem.* **2019**, *43*, 12004−12012.

(22) Liu, Q.; Su, X.; Lei, D.; Qin, Y.; Wen, J.; Guo, F.; Wu, Y.; Rong, Y.; Kou, R.; Xiao, X.; Aguesse, F.; Bareño, J.; Ren, Y.; Lu, W.; Li, Y. Approaching the capacity limit of lithium cobalt oxide in lithium ion

batteries via lanthanum and aluminium doping. *Nat. Energy* **2018**, *3*, 936−943.
(23) Xiao, Z. W.; Zhang, Y. J.; Wang, Y. F. Synthesis of high-capacity $LiNi_{0.8}Co_{0.1}Mn_{0.1}O_2$ cathode by transition metal acetates. *Trans. Nonferrous Met. Soc. China* **2015**, *25*, 1568−1574.
(24) Trevisanello, E.; Ruess, R.; Conforto, G.; Richter, F. H.; Janek, J. Polycrystalline and Single Crystalline NCM Cathode Materials—Quantifying Particle Cracking, Active Surface Area, and Lithium Diffusion. *Adv. Energy Mater.* **2021**, *11*, 2003400.
(25) Zhang, M.; Shen, J.; Li, J.; Zhang, D.; Yan, Y.; Huang, Y.; Li, Z. Effect of micron sized particle on the electrochemical properties of nickel-rich $LiNi_{0.8}Co_{0.1}Mn_{0.1}O_2$ cathode materials. *Ceram. Int.* **2020**, *46*, 4643−4651.
(26) Lin, S. P.; Fung, K. Z.; Hon, Y. M.; Hon, M. H. Effect of Al addition on formation of layer-structured $LiNiO_2$. *J. Solid State Chem.* **2002**, *167*, 97−106.
(27) Lei, T.; Li, Y.; Su, Q.; Cao, G.; Li, W.; Chen, Y.; Xue, L.; Deng, S. High-voltage electrochemical performance of $LiNi_{0.5}Co_{0.2}Mn_{0.3}O_2$ cathode materials via Al concentration gradient modification. *Ceram. Int.* **2018**, *44*, 8809−8817.
(28) Zhang, S. S.; Xu, K.; Jow, T. R. Electrochemical impedance study on the low temperature of Li-ion batteries. *Electrochim. Acta* **2004**, *49*, 1057−1061.
(29) Li, Y. C.; Zhao, W. M.; Xiang, W.; Wu, Z. G.; Yang, Z. G.; Xu, C. L.; Xu, Y. D.; Wang, E. H.; Wu, C. J.; Guo, X. D. Promoting the electrochemical performance of $LiNi_{0.8}Co_{0.1}Mn_{0.1}O_2$ cathode via $LaAlO_3$ coating. *J. Alloys Compd.* **2018**, *766*, 546−555.

https://doi.org/10.1021/acsomega.1c01552
ACS Omega 2021, 6, 16465−16471